Evidence for a Proximal Histidine Interaction in the Structure of Cytochromes *c*′ in Solution: A Resonance Raman Study

Samya Othman,[‡] Pierre Richaud,[§] André Verméglio,[§] and Alain Desbois*[,‡]

Section de Biophysique des Protéines et des Membranes, Département de Biologie Cellulaire et Moléculaire, CEA et CNRS-URA 1290, Centre d'Etudes de Saclay, F-91191 Gif-sur-Yvette Cedex, France, and Section de Bioénergétique Cellulaire, Département de Physiologie Végétale et Ecosystèmes, Centre d'Etudes Nucléaires de Cadarache, F-13108 Saint-Paul-les-Durance, France

Received November 28, 1995; Revised Manuscript Received March 18, 1996[⊗]

ABSTRACT: Soret-excited resonance Raman (RR) spectra of oxidized and reduced cytochromes *c*′ from *Rhodospirillum molischianum* and *Rhodobacter sphaeroides*, in solution, are reported. The spectra of the type I ferricytochromes *c*′ in both species contain different extents of two forms. One of these is readily assignable to a "normal" five-coordinated high-spin heme. The second species with ν_3 and ν_{10} modes at 1502 and 1635 cm^{-1}, respectively, is attributed to a five-coordinated intermediate-spin heme. The RR data show that the equilibrium between these two forms is species-dependent at neutral pH and 20 °C. The ν(Fe−His) mode of the a form of reduced cytochromes *c*′ is assigned to a band at 228−231 cm^{-1}, indicating that the proximal His has a strong electronegative character. X-ray crystallographic data on *R. molischianum* ferricyt *c*′ show that the proximal His has no interaction with either the protein or water molecules [Finzel, B. C., Weber, P. C., Hardman, K. D., & Salemme, F. R. (1985) *J. Mol. Biol. 186*, 627−643]. Considering that the absence of H bonding at the coordinated histidine corresponds to a low frequency for the ν(Fe−His) mode (195−205 cm^{-1}), the structure and/or environment of the proximal histidine appears different for cyt *c*′(III) in the crystal and cyt *c*′(II) in aqueous solution. To account for the elevated frequency of the ν(Fe−His) mode of cyt *c*′(II), several possibilities have been examined. Among these, we propose that a conserved Lys residue, located in the protein sequence three residues before the His ligand, can form an electrostatic interaction with the (His)N_1 atom, directly or through a water molecule. It is further suggested that this electrostatic interaction could also play a role in the high-spin ↔ intermediate-spin equilibrium of oxidized cytochromes *c*′.

Cytochromes *c*′ (cyt *c*′)[1] are soluble monomeric or dimeric proteins extracted from photosynthetic, denitrifying, and nitrogen bacteria (Meyer & Kamen, 1982). The precise biological function of these hemoproteins is not clearly established, although it has been recently suggested that they could be involved in the metabolism of nitrogen (Yamanaka, 1992). The redox potential of cyt *c*′ has been determined in a mid range, varying from −10 to +100 mV (Meyer & Kamen, 1982; Moore & Pettigrew, 1990; Yamanaka, 1992). Numerous spectroscopic techniques have been used to study cyt *c*′. Among these, electronic absorption (Horio & Kamen, 1961; Imai et al., 1969a), electron paramagnetic resonance (EPR) (Ehrenberg & Kamen, 1982; Maltempo, 1974), Mössbauer (Moss et al., 1968), resonance Raman (RR) (Strekas & Spiro, 1974; Kitagawa et al., 1977; Hobbs et al., 1990), magnetic circular dichroism (MCD) (Rawlings et al., 1977), extended X-ray absorption fine structure (EXAFS) (Korszun et al., 1989), and nuclear magnetic resonance (NMR) (Emptage et al., 1981; Moore et al., 1982; La Mar et al., 1990; Bertini et al., 1990; Banci et al., 1992) studies have shown an unusual pH dependence of the electronic structure of heme. Three spectroscopic types have been characterized for oxidized cyt *c*′. Numbered I−III, they correspond to forms observed at pH ca. 7, 10, and 12, respectively (Imai et al., 1969a; Barakat & Strekas, 1982). The spin state of the heme iron of type I is either high, intermediate, or both, depending on the spectroscopy used to investigate the ferricyt *c*′. MCD and NMR studies concluded a pure high-spin (HS) heme structure for all type I cyt *c*′(III) but *Chromatium vinosum* ferricyt *c*′ (Rawlings et al., 1977; La Mar et al., 1990). EPR, EXAFS, and Mössbauer spectroscopies, as well as magnetic susceptibility measurements, showed that type I cyt *c*′(III) represents a quantum admixture of high- and intermediate-spin (IS) states ($S = {}^5/_2, {}^3/_2$) (Moss et al., 1968; Maltempo, 1974; Korszun et al., 1989; Monkara et al., 1992). Finally, the high-frequency regions of RR spectra of type I cyt *c*′(III) from *Rhodopseudomonas palustris*, *Rhodospirillum rubrum*, and *C. vinosum* are anomalous since the spin state sensitive modes appear as single bands and have frequencies close to those of six-coordinated (6c) low-spin (LS) heme derivatives (Strekas & Spiro, 1974; Kitagawa et al., 1977; Hobbs et al., 1990). On the other hand, the electronic structure of types II and III ferricyt *c*′ is unambiguous, corresponding to a pure HS and LS configuration, respectively (Imai et al., 1969a).

* Author to whom correspondence should be addressed.
[‡] CEA et CNRS-URA 1290.
[§] Centre d'Etudes Nucléaires de Cadarache.
[⊗] Abstract published in *Advance ACS Abstracts,* June 15, 1996.
[1] Abbreviations: ArP, *Arthromyces ramosus* peroxidase; CcP, cytochrome *c* peroxidase; CD, circular dichroism; CiP, *Coprinus cinereus* peroxidase; Cyt, cytochrome; EPR, electron paramagnetic resonance; EXAFS, extended X-ray absorption fine structure; ferricyt *c*′ or cyt *c*′(III), oxidized cytochrome *c*′; ferrocyt *c*′ or cyt *c*′(II), reduced cytochrome *c*′; HS, high-spin; IS, intermediate-spin; LiP, lignin peroxidase; LS, low-spin; Mb, myoglobin; MCD, magnetic circular dichroism; MP8, microperoxidase-8; NMR, nuclear magnetic resonance; RR, resonance Raman; 5c, five-coordinated; 6c, six-coordinated.

S0006-2960(95)02818-2 CCC: $12.00

The interconversion of these three forms is reversible, but only the type I → type II transition maintains the secondary protein structure (Imai et al., 1969b; Emptage et al., 1981).

As far as the ferrocytochromes *c*′ are concerned, they exhibit two forms called "a" and "n". The former is detected at neutral pH. Its heme adopts a HS five-coordinated (5c) structure (Ehrenberg & Kamen, 1965; Moss et al., 1968; Strekas & Spiro, 1974; Kitagawa et al., 1977). Observed at very alkaline pH, the n form is 6cLS and appears to be similar to the coordination and spin states of most ferrous *c*-type cytochromes (Kamen & Horio, 1970).

The three-dimensional structure of oxidized cyt *c*′ from *Rhodospirillum molischianum*, *R. rubrum*, and *C. vinosum* has been solved (Weber et al., 1981; Finzel et al., 1985; Yasui et al., 1992; Ren et al., 1993). They all show a dimeric structure composed of two cyt *c*′ stabilized by ionic and hydrophobic interactions. Each cyt *c*′ monomer is composed of four left-twisted and antiparallel α helices. The heme is linked to the C-terminal helix by the specific Cys-X-Y-Cys-His sequence of most *c*-type cytochromes. Its proximal site is occupied by the His residue of this conserved sequence, whereas the sixth coordination site is vacant. Contrary to most hemoproteins for which a three-dimensional structure is known, the crystallographic data on cyt *c*′ indicate that the proximal His does not interact with any amino acid side chain or the backbone of the protein. Although exposed to the solvent, this His residue has no structured water molecules in its proximity (Finzel et al., 1985). This result is controversial since it does not account for the pH sensitivity of cyt *c*′ (Moore et al., 1985; Moore & Pettigrew, 1990). Actually, the authors proposed that the proximal His might be deprotonated and the resulting histidinate group stabilized by an ionic interaction with a protein residue.

In order to understand several problematic aspects of the heme properties of cyt *c*′, we have used RR spectroscopy and studied the cyt *c*′ extracted from two non-sulfur purple photosynthetic bacteria, i.e. *Rhodobacter sphaeroides* and *R. molischianum*. The choice of the *R. molischianum* cyt *c*′ was governed by the fact that its crystal structure is solved at a 1.67 Å resolution (Finzel et al., 1985). On the other hand, RR spectroscopy is a powerful technique yielding information about the structure and environment of heme(s) buried in hemoproteins (Kitagawa & Ozaki, 1987; Spiro & Li, 1988; Kitagawa, 1988; Desbois, 1994). The RR spectra of cyt *c*′ will be compared to those obtained from RR studies performed on various complexes of microperoxidase-8 (MP8) (Othman et al., 1993, 1994; Othman, 1994). Indeed, this latter heme *c*−octapeptide system was recently used to model the active sites of various *c*-type cytochromes.

EXPERIMENTAL PROCEDURES

Protein Purification. *R. molischianum* and *R. sphaeroides* cells were grown in white light under anaerobic conditions. The strain D120 of *R. molischianum* was grown in a modified Hunter milieu, according to Gemeroth (1993). *R. molischianum* and *R. sphaeroides* cyt *c*′ have been prepared according to Meyer and Cusanovich (1985). In the 6.8−8.0 pH range, the hemoproteins (∼20 μM) were studied in either 50 mM Tris-HCl or 50 mM potassium phosphate buffer. For the alkaline form of cyt *c*′, a 100 mM sodium carbonate (pH 12) buffer was used. The cytochromes were reduced by addition of solid sodium dithionite under anaerobic conditions (Othman et al., 1993, 1994). The UV−visible absorption spectra of oxidized and reduced cyt *c*′ were recorded at various pHs on a Beckman DU7 or Shimadzu UV160 spectrophotometer. These spectra exhibited no significant differences with respect to those previously published (Moore et al., 1982; Meyer & Cusanovich, 1985).

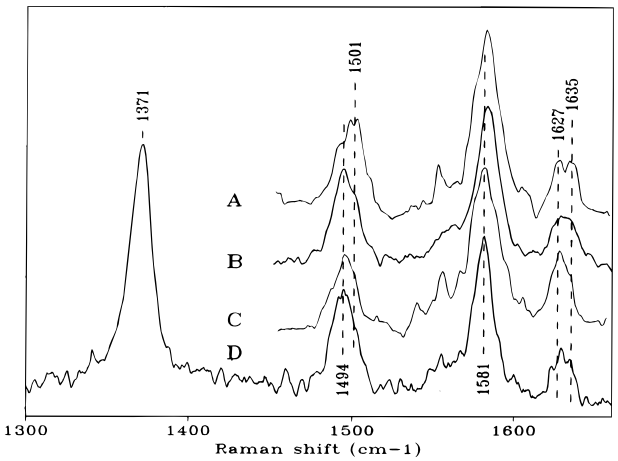

FIGURE 1: High-frequency regions of resonance Raman spectra of oxidized cytochrome *c*′ from *R. molischianum*: (A) pH 6.8 and 413.1 nm excitation, (B) pH 6.8 and 406.7 nm excitation, (C) pH 8.0 and 413.1 nm excitation, and (D) pH 8.0 and 406.7 nm excitation; summation of six scans.

Resonance Raman Spectra. RR spectra were excited with the 441.6 (Liconix He-Cd, model 4240N) and 406.7 and/or 413.1 nm (Coherent Innova Kr^+) laser beams and were recorded using a Jobin-Yvon spectrometer (HG2S-UV). Radiant powers of 10−30 mW were used. Improvement of the signal-to-noise ratios of RR spectra was achieved by summations of two to eight scans. The band positions and intensities were determined by use of band-fitting programs (Spectra Calc, Galactic Industries) (Othman et al., 1994). Under these conditions, the frequency precision is 0.5−2 cm^{-1} depending on both the band intensity and the signal-to-noise ratio. All the spectra were recorded at 20 (±1) °C.

RESULTS

High-Frequency Regions of Resonance Raman Spectra of Oxidized Cytochromes c′

The high-frequency regions (1280−1680 cm^{-1}) of RR spectra of oxidized cyt *c*′ from *R. molischianum*, excited at 413.1 and 406.7 nm, are presented in Figure 1. At pH 6.8, the 413.1 nm-excited spectrum shows a main contribution at 1501 cm^{-1} for the ν_3 mode and two distinct bands at 1627 and 1635 cm^{-1} for ν_{10}. The ν_4 and ν_2 modes correspond to single bands observed at 1371 and 1582 cm^{-1}, respectively (Figure 1A, Table 1). On the other hand, the spectrum excited at 406.7 nm exhibits a main component at 1494 cm^{-1} for the ν_3 mode and a broad unresolved band at 1631 cm^{-1} for ν_{10}. When the pH value is increased (pH 8), a weakening of the 1501 and 1635 cm^{-1} bands is detected, especially in the RR spectra excited at 413.1 nm (Figure 1). Therefore, type I cyt *c*′(III) from *R. molischianum* exhibits two components for the spin state sensitive modes ν_3 and ν_{10}, reflecting a mixture of two heme structures.

The RR experiments on *R. sphaeroides* cyt *c*′(III) at pH 7.2 show a different pattern. Indeed, the 1502 and 1635 cm^{-1} bands constitute the major features in the ν_3 and ν_{10} regions

Table 1: High-Frequency Raman Modes (cm^{-1}) of Various Ferricytochromes c' at pH 6.8−8.0[a]

cyt c'	*R. molischianum*		*R. sphaeroides*	*R. palustris* (a)	*R. rubrum* (b)	*C. vinosum* (c)
pH	6.8	8.0	7.2	6.9	7.3	7.0
excitation (nm)	407/413		407/413	488	514	407
υ_{21}		1317	1310	1315	1313	
υ_4	1371	1370	1371	1372	1373	1371
υ_{20}					1409	
υ_3	1494	1495	1490			
	1501		1502	1500		1502
υ_{38}	1553	1553	1551			
υ_{11}		1558	1558	1559	1558	
υ_{19}				1578	1577	
υ_2	1581	1580	1582	1581	1582	1580
υ_{37}	1605					
υ_{10}	1627	1625	1628			
	1635		1635	1637	1637	1637

[a] The RR data are from (a) Strekas and Spiro (1974), (b) Kitagawa et al. (1977), and (c) Hobbs et al. (1990).

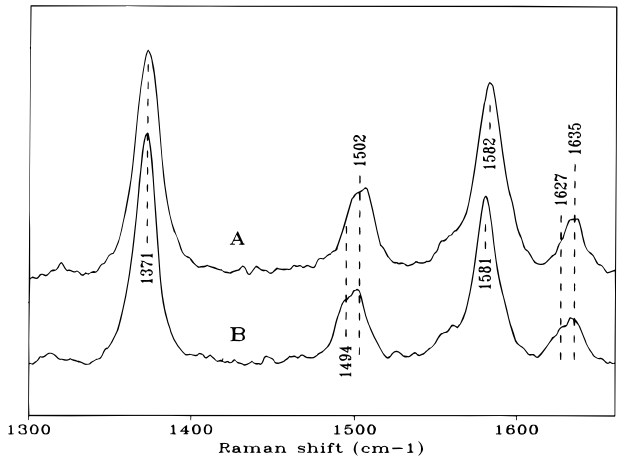

FIGURE 2: High-frequency regions of resonance Raman spectra of oxidized cytochrome c' from *R. sphaeroides*: (A) pH 7.2 and 413.1 nm excitation and (B) pH 7.2 and 406.7 nm excitation; summation of six scans.

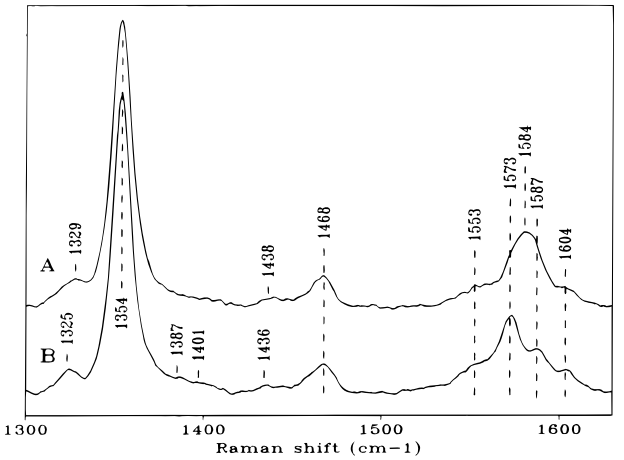

FIGURE 3: High-frequency regions of resonance Raman spectra of reduced cytochromes c': (A) cyt c' from *R. molischianum* at pH 8.0 and (B) cyt c' from *R. sphaeroides* at pH 8.0; excitation at 441.6 nm, summation of six scans.

of RR spectra excited at either 413.1 or 406.7 nm (Figure 2). Therefore, a different two-state equilibrium is detected for *R. molischianum* and *R. sphaeroides* ferricyt c' at neutral pH and 20 °C.

Both Figures 1 and 2 indicate that the 1501−1502 and 1635 cm^{-1} components are best enhanced with 413.1 nm excitation. On the contrary, the 1494 and 1627 cm^{-1} components appear relatively enhanced with 406.7 nm excitation. Moreover, one can note a different behavior in the changes in relative intensities of the υ_3 and υ_{10} modes with these excitations. Since these modes are of different symmetry, this effect simply reflects differences in the resonance conditions of the 1494, 1501, 1627, and 1635 cm^{-1} bands (Spiro, 1983; Kitagawa, 1988).

High-Frequency Regions of Resonance Raman Spectra of Reduced Cytochromes c′

Type a Ferrocytochrome c′. Figure 3 displays the high-frequency RR spectra of the a form of reduced cyt c' from *R. molischianum* and *R. sphaeroides* at neutral pH. The frequencies of υ_3, υ_4, and υ_{10} modes are identical for both species (1468, 1354, and 1604 cm^{-1}, respectively) (Table 2). The same sets of frequencies were previously found for 5cHS complexes of ferrous MP8 (Othman et al., 1993). These comparisons confirm the 5cHS heme configuration of type a cyt c'(II). Nevertheless, the ferrocyt c' spectra exhibit striking frequency differences in the 1560−1590 and 1320−1330 cm^{-1} regions (Figure 3). In the latter region, a broad band observed at 1329 cm^{-1} in the *R. molischianum* spectrum is apparently downshifted to 1325 cm^{-1} in the spectrum of *R. sphaeroides*. This region contains two overlapping bands corresponding to a stretching mode of C_m−H (υ_{21}) and a deformation mode of the thioether groups (Hu et al., 1993). Thus, the frequency variations of the 1325−1329 cm^{-1} band reflect some peripheral changes in the heme−protein interactions between *R. sphaeroides* and *R. molischianum* cyt c'(II).

In the 1570−1590 cm^{-1} regions of RR spectra of *R. sphaeroides* cyt c'(II), two well-resolved bands are detected at 1573 and 1587 cm^{-1} (Figure 3). In the spectra of *R. molischianum* cyt c'(II), changes in intensities and/or in frequencies of these two bands are observed as compared to those of *R. sphaeroides*; the 1587 cm^{-1} band seems to be downshifted to 1584 cm^{-1} in increasing its relative intensity, while the 1573 cm^{-1} band appears relatively weaker. The 1573 and 1584 cm^{-1} bands were assigned to the υ_2 and υ_{37} modes, respectively (Othman et al., 1993). In the RR spectra of 5cHS ferrous MP8 complexes, the υ_2 mode is seen at 1571−1572 cm^{-1} whereas the υ_{37} mode is variable in both frequency (1584−1588 cm^{-1}) and relative intensity (Othman et al., 1993). An even larger frequency dispersion of the

Table 2: High-Frequency Raman Modes (cm^{-1}) of Various Ferrocytochromes *c*′[a]

cyt *c*′	*R. molischianum*	*R. sphaeroides*		*R. palustris* (a)		*R. rubrum* (b)		*C. vinosum* (c)	
type	a	a	n	a	n	a	n	a	n
excitation (nm)	413/442	413/442	413	514	514	514	514	407	407
υ_{21}	1317	1314	1316	1320	1315	1319	1314		
$\delta(C_a-R)$	1329	1325							
υ_4	1354	1354	1358	1355	1360	1355	1360	1352	1358
υ_{29}	1402		1396	1403	1402	1402	1399	1401	
υ_{20}	1438	1436							
υ_{28}	1459	1459							
υ_3	1468	1468	1496	1475		1472	1494	1469	1488
υ_{11}	1553	1550	1535	1550	1539	1551	1535		
υ_{19}	1559	1561		1557	1589	1557	1585		
υ_2	1573	1573	1594						1592
υ_{37}	1584	1587		1583		1582		1577	
υ_{10}	1604	1604	1626	1609		1609	1619		

[a] The RR data are from (a) Strekas and Spiro (1974), (b) Kitagawa et al. (1977), and (c) Hobbs et al. (1990).

υ_{37} mode has been previously reported in the RR spectra of 5cHS deoxyhemoproteins (Desbois et al., 1984b). The frequency variations of this porphyrin mode [$\upsilon(C_b-C_b)$] have been associated with changes in the peripheral interaction between heme and protein (Desbois et al., 1984a,b). Thus, the changes observed in both the 1320−1330 and 1570−1590 cm^{-1} regions of RR spectra of cyt *c*′(II) from *R. molischianum* and *R. sphaeroides* reflect differences of the heme environment.

Type n Ferrocytochrome c′. The RR spectrum of *R. sphaeroides* cyt *c*′(II) at pH 12 is typical of a 6cLS complex with υ_4, υ_3, υ_2, and υ_{10} detected at 1358, 1496, 1594, and 1626 cm^{-1}, respectively (Table 2). These frequencies are very similar to those of 6cLS complexes of ferrous MP8 (Othman, 1994; Othman et al., 1994) and of the n form of cyt *c*′(II) from *R. rubrum* and *C. vinosum* (Kitagawa et al., 1977; Hobbs et al., 1990). The υ_{11} frequency which is sensitive to the axial ligation of heme is observed at 1535 cm^{-1} (Table 2). RR studies on various complexes of MP8-(II) associate this frequency with an axial heme ligation of the histidine-amine or histidine-histidinate type (Othman, 1994; Othman et al., 1994).

Low-Frequency Regions of RR Spectra of Ferrocytochromes c′

The 441.6 nm excitation of RR spectra enhances the υ(Fe−His)-involving mode of 5cHS ferrous complexes (Nagai et al., 1980; Desbois et al., 1981; Bangcharoenpaurpong et al., 1984; Kitagawa, 1988; Othman et al., 1993). The low-frequency regions of the 441.6 nm-excited RR spectra from *R. molischianum* and *R. sphaeroides* cyt *c*′(II) are presented in Figure 4. Both spectra exhibit the most prominent band at 228 and 231 cm^{-1} for *R. molischianum* and *R. sphaeroides* cyt *c*′, respectively. This band is also active with 413.1 nm excitation but disappears upon the a → n transition (Figures 4 and 5).

The low-frequency RR spectra of type a ferrocyt *c*′ show important differences in band frequency as well as in relative band intensity in the 250−450 cm^{-1} regions (Figure 4). The bands of these regions being essentially assigned to out-of-plane porphyrin modes and deformation modes of porphyrin side chains (Hu et al., 1993; Desbois, 1994), the spectral differences observed in Figure 4 are again interpreted in terms of variation in peripheral heme−protein interactions.

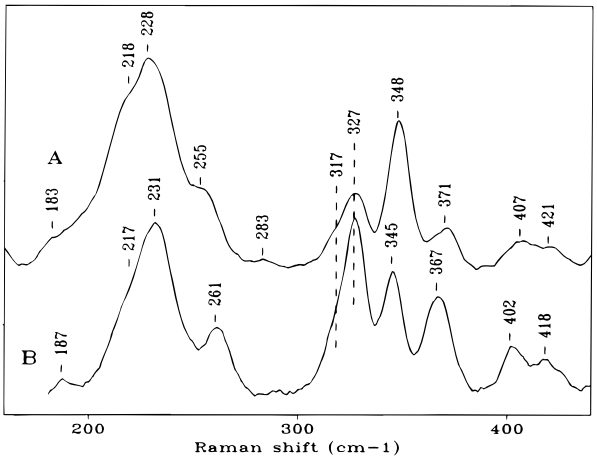

FIGURE 4: Low-frequency regions of resonance Raman spectra of reduced cytochromes *c*′: (A) cyt *c*′ from *R. molischianum* at pH 8.0 and (B) cyt *c*′ from *R. sphaeroides* at pH 8.0; excitation at 441.6 nm, summation of four scans.

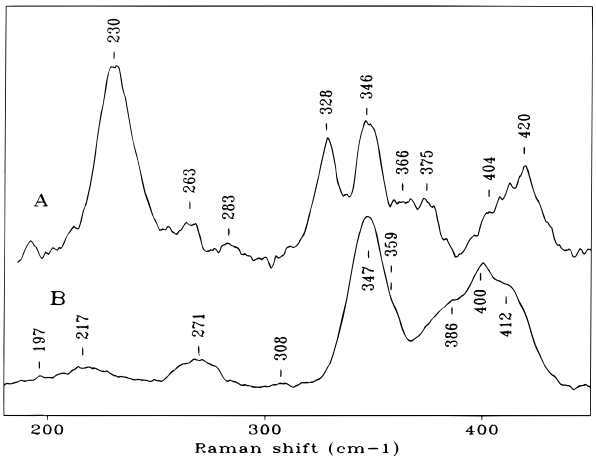

FIGURE 5: Low-frequency regions of resonance Raman spectra of *R. sphaeroides* ferrocytochrome *c*′ at pH 8.0 (A) and 12.0 (B); excitation at 413.1 nm, summation of six scans.

The a → n transition of ferrocyt *c*′ reduces the number of the low-frequency RR bands (Figure 5). This transition, in introducing a sixth ligand to heme, thus appears to decrease the porphyrin symmetry. The spectra of type n cyt *c*′(II) are similar to those of ligated complexes of MP8(II), except the intensity of the 380−420 cm^{-1} bands that is weakened (Othman, 1994; Othman et al., 1994).

DISCUSSION

ν(Fe−His) Mode of Type a Ferrocytochromes c′

Hobbs et al. (1990) recently proposed that a 231 cm^{-1} band could be associated with the ν(Fe−His) mode of *C. vinosum* ferrocyt *c′*. However, this investigation has used a 406.7 nm excitation that is not favorable for the observation of this axial mode (Desbois et al., 1981; Baurcharoenpaurpong et al., 1984; Othman et al., 1993). Moreover, a 232 cm^{-1} band was detected in the RR spectra of ligated forms of cyt *c′*(II) (Hobbs et al., 1990). Thus, all these observations do not fully support the proposed ν(Fe−His) assignment.

Previous studies have demonstrated that 441.6 nm is one of the best excitations to observe the ν(Fe−N(imidazole))-involving mode of 5cHS ferrohemes and ferrohemoproteins containing heme *b* (Nagai et al., 1980; Desbois et al., 1981, 1984a,b; Argade et al., 1984). For 5cHS ferroheme *c* complexes excited at 441.6 nm, this mode has also been characterized as the strongest band in the 50−450 cm^{-1} regions of RR spectra (Othman et al., 1993). Using the same excitation, the most intense band of the low-frequency RR spectra of ferrocyt *c′* is observed at 228−231 cm^{-1} (Figure 4). The strong similarities of RR spectra of ferrocyt *c′*(II) and 5cHS MP8(II) derivatives, excited at 441.6 nm, therefore allow the assignment of the ca. 230 cm^{-1} band to the ν(Fe−N(His)) mode of cyt *c′*(II). However, one may note that 413.1 nm excitation maintains a relatively high intensity for this axial mode (Figures 4 and 5), while it is not the case for the 5cHS MP8(II) complexes (Othman et al., 1993). This particularity could be related to the marked splitting of the Soret band of type a ferrocyt *c′* (Imai et al., 1969a; Meyer & Kamen, 1982; Moore et al., 1982; Meyer & Cusanovich, 1985). The fact that the 230 cm^{-1} band totally disappears upon ligation in sixth-heme coordination supports the ν(Fe−His) assignment (Figure 5). All these observations also validate the proposed assignment of the 231 cm^{-1} RR band of *C. vinosum* cyt *c′*(II) excited at 406.7 nm (Hobbs et al., 1990).

Electronegativity and Environment of the Proximal Histidine in Type a Ferrocyt c′

Electronegative Character of the Proximal Histidine. In the 1.7 Å refined structure of *R. molischianum* cyt *c′*(III), the histidylimidazole group serving as the heme ligand (His 122) is exposed to solvent and its N_1H group is not involved in H bonding with the protein (Finzel et al., 1985). The latter group is also not in H bonding interaction with water, the solvent molecules being too far away (≥3.5 Å) (Finzel et al., 1985). A ν(Fe−His) mode in which the His ligand has either no H bond or a weak H-bonding partner is expected to be observed in a low-frequency region, i.e. at 195−205 cm^{-1} (Smulevich et al., 1988; Othman et al., 1993). A ν(Fe−His) mode at 228−231 cm^{-1}, like that detected for cyt *c′*(II), indicates that the axial histidylimidazole *c′* has a marked electronegative character (Stein et al., 1980; Teraoka & Kitagawa, 1981; Othman et al., 1993; Smulevich et al., 1994b). To account for this high ν(Fe−His) frequency, it is therefore necessary to invoke some differences in the environment or/and the structure of the iron−histidine bond of ferricyt *c′* (in the crystal) and ferrocyt *c′* (in aqueous solution). The electrostatic effect exerted by the protein and/or the solvent on the N_1H group of the heme-bound imidazole

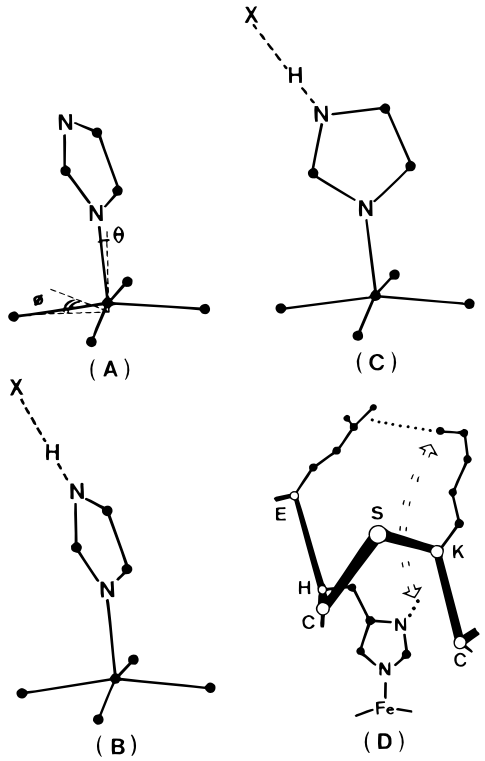

FIGURE 6: Coordination geometry and histidine environment in ferrocytochrome *c′*: (A) no H bond at the (His)N_1 site and bisecting position of the imidazole ring ($\phi = 43°$) (case of the ferricytochrome *c′* crystal), (B) H bond at the (His)N_1 site (X = H_2O, NH_2, or NH_3^+) and bisecting position of the imidazole ring, (C) H bond at the (His)N_1 site (X = H_2O, NH_2, or NH_3^+) and eclipsing position of the imidazole ring ($\phi = 0°$), and (D) schematic representation of a plausible modulation of the hystidylimidazole electronegativity by the side chain conformation of the conserved lysine of cytochromes *c′* [adapted from Ren et al. (1993)].

and the coordination geometry of the FeN_4(pyrrole)−imidazole group are two main factors that influence the ν(Fe−His) frequency. To explain the origin of the 230 cm^{-1} frequency of type a cyt *c′*(II), several hypotheses considering these two parameters are envisaged in the following.

H Bonding Interaction between the Proximal Histidine and Water. In opposition to the situation observed in the cyt *c′*(III) crystal structure (Figure 6A), one might first assume that the proximal His of cyt *c′*(II) in solution could interact with water molecule(s) (Figure 6B). Examples of H bonding interaction between heme-coordinated imidazole and water molecule(s) are relatively scarce. A water molecule involved in a H bond with an imidazole bound to a ferriheme has been detected in the X-ray structure of a bis(imidazole) complex of Fe(III)−tetraphenylporphyrin (Scheidt et al., 1987). In fact, this (imidazole)N_1H-H_2O interaction constitutes a part of a hydrogen bond network in which the water molecule is stabilized by two chloride anions. In the crystallographic structure of various tetraheme ferricytochromes c_3, similar imidazole−H_2O interactions have been observed (Morais et al., 1995, and references therein). Three of the eight histidylimidazole ligands are indeed each H bonded by a single water molecule. In these cases, the solvent molecule is also included in a H bond network. However, it is stabilized by two carbonyl groups, originating from either a glutamine side chain, a glutamic acid side chain, or, most frequently, the polypeptide backbone. The (imidazole)N_1−O(water) distances are 2.7−3.0 Å (Scheidt et al.,

1987; Morais et al., 1995). Those corresponding to a (imidazole)N_1−O(carbonyl peptide) interaction appear, on average, shorter (2.5−2.9 Å), suggesting that the electrostatic effect of a stabilized water molecule is nearly equivalent to or even slightly weaker than that exerted by a peptide carbonyl group.

One may add that these imidazole−H_2O interactions have been seen for ligands bound to ferrihemes. Since the polarizability of the N_1H group is strongly decreased by reduction of the heme iron (Sundberg & Martin, 1974; Desbois & Lutz, 1992), the electropositivity and thus the H bond donor power of the N_1 proton is decreased by this change in oxidation state of the heme iron. Therefore, the affinity of water molecules and carbonyl peptide groups to the N_1 proton of the proximal histidylimidazole of hemoproteins is expected to be similar but largely decreased in passing from the oxidized to the reduced state.

The Fe(II)PP(2MeImH) complex in aqueous solution exhibits a υ(Fe−2MeImH) mode at 219−220 cm^{-1} (Stein et al., 1980; Hori & Kitagawa, 1980; Teraoka & Kitagawa, 1981; Desbois & Lutz, 1981; Ondrias et al., 1982). Considering that both mammalian deoxymyoglobins exhibit a υ(Fe−His) mode at 220−222 cm^{-1} and the near equivalence of the electrostatic effect on the N_1H(imidazole) group of a water molecule and a carbonyl group, the above Fe(II)PP(2MeImH) model could be retained as representative of a 5cHS ferrous system in which the axial imidazole ring might interact with water molecule(s). On the basis of a downshift of the 219−220 cm^{-1} band to 205−206 cm^{-1} when the Fe(II)PP(2MeImH) complex is dispersed in an aqueous detergent, it has been assumed that the ca. 14 cm^{-1} shift corresponds to a change in H bonding interaction of the N_1H group of 2MeImH (Hori & Kitagawa, 1980; Teraoka & Kitagawa, 1981). More precisely, it has been suggested that the micelle formation could block interactions of the bound 2MeImH with water molecules, causing a change in the Fe−ligand bond strength (Hori & Kitagawa, 1980; Stein et al., 1980; Teraoka & Kitagawa, 1981). In fact, the downshift of the υ(Fe−ligand) mode of Fe(II)PP(2MeImH) is accompanied by a red shift of the Soret band from 425 to 431 nm (Desbois & Lutz, 1981). For the 1,2-dimethylimidazole complex of Fe(II)PP, in which H bonding at the N_1 site is precluded, a similar effect is detected. The Soret band is red shifted by 6 nm (Desbois & Lutz, 1981). The axial mode is downshifted from 199−200 to 193−194 cm^{-1} (Desbois & Lutz, 1981; Ondrias et al., 1982). Therefore, all these spectral changes cannot be primarily interpreted as reflecting a change in H bonding of the N_1H group. Changes in the coordination geometry of the FeN_4(pyrrole)−2MeImH group would rather occur when the Fe(II)−porphyrin complexes interact with the micelle.

Some H bonding between the bound 2MeImH and the solvent H_2O cannot be totally excluded in the case of Fe(II)PP(2MeImH) in water. However, the 2MeImH excess, the dithionite excess used for the heme reduction, and the oxidation products of dithionite, as well as the counterion of the hemin serving to prepare the ferroheme complex (generally Cl^-), are all able to form strong H bond(s) with the 2MeImH liganded to ferroheme. Thus, a Fe(II)−porphyrin−imidazole system in which only water molecules interact with the imidazole ligand remains to be characterized.

Conformation of the FeN_4(pyrrole)−Imidazole Group. The electronegativity of the axial imidazole is the main determinant in the frequency of the υ(Fe−axial ligand) mode (Othman et al., 1993). However, geometrical factors such as the out-of-plane displacement of the iron atom relative to the FeN_4(pyrrole) plane, the tilting of the Fe−N(imidazole) bond off the normal to the FeN_4(pyrrole) plane, and the position of the imidazole plane relative to the N(pyrrole)−Fe−N(pyrrole) axes are expected to modulate the axial mode frequency (Bancharoenpaurpong et al., 1984; Stavrov, 1993). Recently, Smulevich et al. (1994b) pointed out the strong influence of the imidazole rotation on the υ(Fe−ligand) mode. This structural parameter is generally estimated from the value of the dihedral angle ϕ formed by the imidazole plane and the nearest N(pyrrole)−Fe−N(pyrrole) axis. The strong effect of ϕ on the υ(Fe−His) mode likely relies on the fact that, in hemoproteins, the iron atom displacement as well as the tilting angle of the axial bond have limited variations (0.3−0.55 Å and 0−11°, respectively) while the imidazole rotation can fully vary ($0° \leq \phi \leq 45°$) (Finzel et al., 1984, 1985; Bolognesi et al., 1989; Evans & Brayer, 1990; Oldfield et al., 1992).

In bis(imidazole) complexes of Fe(III)−porphyrin, the conformers with the smallest ϕ angles are thermodynamically favored (Scheidt et al., 1987). Inspection of the structure of Fe(II)−porphyrin−imidazole complexes indicates the same trend with an averaged ϕ value of 7° (Jameson et al., 1980; Hoard, 1985; Scheidt et al., 1985, 1987; Momenteau et al., 1988). For most mammalian myoglobin (Mb), in which the histidylimidazole plane nearly eclipses two Fe−N(pyrrole) bonds ($\phi = 0°$) (Evans & Brayer, 1990; Oldfield et al., 1992), the υ(Fe−His) mode is detected at 220−222 cm^{-1} (Desbois et al., 1981; Kitagawa, 1988; Spiro & Li, 1988). Structural investigations have shown that, for a similar tilting of the Fe−His bond ($\Theta = 3-4°$), the ϕ angle is increased to 29 and 40° in *Aplysia limacina* myoglobin and *Scapharca inaequivalvis* hemoglobin, respectively (Bolognesi et al., 1989; McGourty et al., 1989). The corresponding frequencies for the υ(Fe−His) mode have been determined at 210 and 203 cm^{-1} (Desbois et al., 1981; Song et al., 1993). A rough linear correlation between these three υ(Fe−His) frequencies and the ϕ angles thus predicts a frequency downshift of −0.4 cm^{-1} per degree for the υ(Fe−His) mode (Figure 7). A similar situation apparently occurs when the fifth ligand exhibits a histidinate character. Similar distances between the N_1 atom and a carboxylate group have been observed in the crystal structure of cytochrome *c* peroxidase (CcP), lignin peroxidase (LiP), and fungal peroxidases (CiP and ArP) (Finzel et al., 1984; Poulos et al., 1993; Kunishima et al., 1994; Petersen et al., 1994). The υ(Fe−His) mode was observed at ca. 247, 244, and 230 cm^{-1}, respectively (Kuila et al., 1985; Hashimoto et al., 1986; Dasgupta et al., 1989; Mylrajan et al., 1990; Smulevich et al., 1988, 1994b). Here again, an increase in ϕ leads to a decrease in the υ(Fe−His) stretch frequency since, for a small value for the Θ angle (3−6°), the imidazole rotation is increased from 14° in CcP and LiP to 40° in fungal peroxidases (Finzel et al., 1984; Poulos et al., 1993; Kunishima et al., 1994) (Figure 7). This change represents a shift of the υ(Fe−His) frequency of −0.7 cm^{-1} per degree of imidazole rotation.

In cyt *c*′(III), the histidylimidazole ring nearly bisects the Fe−N(pyrrole) bonds ($\phi = 43°$) (Finzel et al., 1985; Yasui et al., 1992). Therefore, the preceding observations would suggest that this imidazole orientation strongly reduces the

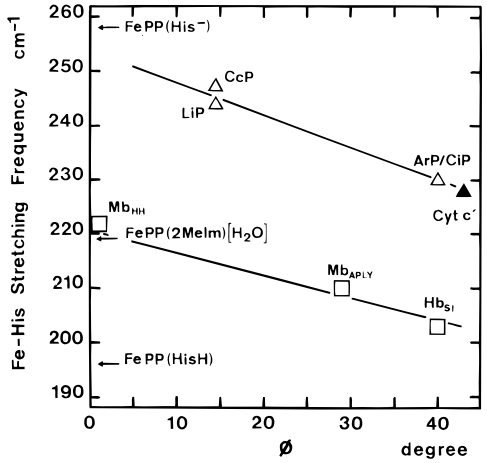

FIGURE 7: ϕ dependence of the υ(Fe−N(imidazole)) mode of 5cHS ferrous heme complexes [structural data from Finzel et al. (1984, 1985), Bolognesi et al. (1989), McGourty et al. (1989), Poulos et al. (1993), and Kunishima et al. (1994); Raman data from Desbois et al. (1981), Kuila et al. (1985), Hashimoto et al. (1986), Smulevich et al. (1988, 1994b), Dasgupta et al. (1989), Mylrajan et al. (1990), and Song et al. (1993)].

effect of the His electronegativity on the υ(Fe−His) frequency (Figure 7). From the above estimations between the υ(Fe−His) frequencies and ϕ values of oxygen carriers and peroxidases, an extrapolation to $\phi = 0$ would give a "corrected" frequency of 248−261 cm^{-1} for the υ(Fe−His) mode of cyt *c*′(II). This frequency range includes the frequency of the Fe(II)PP(histidinate) complex (258 cm^{-1}) (Othman et al., 1993) (Figure 7) and confirms the anionic character of the proximal His of cyt *c*′(II). However, in the frame of our starting hypothesis, the assumed N_1H(His)−H_2O interaction in cyt *c*′(II) would have to be transformed into a N_1(histidinate)−H_2O interaction considering the above extrapolation to ϕ_0. This latter situation is unlikely since the imidazolate formation is not compatible with the presence of water in its N_1H proximity (Stein et al., 1980; Teraoka & Kitagawa, 1981).

Therefore, this first hypothesis, considering both a (His)-N_1H−H_2O hydrogen bond and bisecting position of the histidylimidazole ring (Figure 6B), is hardly plausible to account for the 228−231 cm^{-1} frequency of cyt *c*′.

Proximal His−H_2O Interaction and Change in Orientation of the Imidazole Ring. With respect to the preceding situation that maintains the geometry of the FeN_4(pyrrole)−histidine group of cyt *c*′(III), a second hypothesis would be that a (His)N_1H−H_2O interaction takes place in the structure of reduced cyt *c*′, but with a decreased ϕ angle (Figure 6C). Assuming that the 220 cm^{-1} frequency of Fe(II)PP(2MeImH) in water is indicative of a ligand−H_2O H bonding interaction and considering that the imidazole rings of the 5cHS ferroporphyrin complexes are nearly eclipsed ($\phi \sim 7°$) (Jameson et al., 1980; Hoard, 1985; Scheidt et al., 1985, 1987; Momenteau et al., 1988), the 230 cm^{-1} frequency could be explained by this hypothesis. Some increases in the Fe−His bond strength could be expected if the water molecule were structured by the protein environment. In reference to the cyt *c*′(III) structure (Weber, 1982; Finzel et al., 1985), this scheme suggests some protein reorganization around the proximal His to allow both an imidazole rotation and a water interaction.

The comparison of the X-ray structures of various *c*-type cytochromes shows that the backbone folding of the Cys-X-Y-Cys-His motif of cyt *c*′ is different from that of most *c*-type cytochromes (Finzel et al., 1985). This structural variation is at the origin of different heme and histidine orientations with respect to the Cys-X-Y-Cys α helix. In particular, the imidazole ring of proximal His is rotated by ca. 90° in the cyt *c*′ structure (Finzel et al., 1985). Therefore, a modification of the imidazole ring position can be regulated by the conformation of the Cys-X-Y-Cys-His backbone of cyt *c*′. On the other hand, the water molecule needs some stabilization by electronegative protein groups, taking into account the known (imidazole)N_1H−H_2O interactions (Scheidt et al., 1987; Morais et al., 1995). An inspection of the structure of the proximal side of the heme pocket of cyt *c*′ shows two lysyl side chains (Lys 119 and 126) pointing toward the histidylimidazole ring (Weber, 1982; Finzel et al., 1985). In addition to carbonyl peptide groups, glutamic residues in position 123 and 124 could participate in a H bond network with water molecule(s). Given the location of the heme binding site in a flexible protein portion, the flexibility of the lysyl chains, the ability of the N amino group of Lys to accommodate water molecules, as well as possible changes in the conformation of the Cys-X-Y-Cys-His motif and in the position of the imidazole ring (Weber, 1982; Finzel et al., 1985; Ren et al., 1993; Richardson & Richardson, 1989), this second hypothesis appears more plausible than the preceding.

c-type motif	-C-X-Y-C-H-
CYTOCHROME c'	Heme
R. molischianum	-C-K-A-C-H-E-E-F-K-Q-D
C. vinosum	-C-K-S-C-H-E-K-Y-R-A-K
R. sphaeroides	-C-K-S-C-H-D-D-F-R-V-K-R

FIGURE 8: Partial sequence alignment of the C-terminal end of *R. molischianum*, *C. vinosum*, and *R. sphaeroides* cytochromes *c*′ [from Ambler et al. (1981) and Ren et al. (1993)].

Direct Ionic Interaction between the Proximal Histidine and a Basic Protein Residue. To account for the low pK_a values of the type I → type II transition of cyt *c*′(III) in solution, Moore et al. (1985) suggested that a basic amino acid side chain could interact with the axial histidine to stabilize it under an imidazolate form. This model differs from the preceding by the direct interaction of the basic residue with the proximal His, and not through a water molecule (Figure 6C). This hypothesis also appears compatible with the results of our RR investigation on type a cyt *c*′(II). A υ(Fe−His) frequency at 228−232 cm^{-1} is indeed in accordance with a histidinate ligand interacting with a charged protein residue whatever the ϕ value (Othman et al., 1993; Smulevich et al., 1994b). For a ϕ value analogous to that observed in cyt *c*′(III) ($\phi = 43°$), this frequency would represent a strong imidazolate character (Smulevich et al., 1994b) (Figure 7). For a ϕ angle close to 0°, the imidazolate character of the proximal His would be weaker. In the structure of cyt *c*′(III), one of the two basic residues in close proximity with the proximal side of heme could play a role in a histidinate stabilization (Moore et al., 1985). It could be the completely conserved Lys residue found in the protein sequence three residues before the heme ligand, i.e. in the X position of the Cys-X-Y-Cys-His motif (Figure 8). Alternatively, it could be either an Arg or a Lys side chain

Table 3: Low-Frequency Raman Modes (cm^{-1}) of Ferrocytochromes *c*′ from *R. molischianum*, *R. sphaeroides*, and *C. vinosum*

cyt *c*′	*R. molischianum*	*R. sphaeroides*		*C. vinosum*[a]
type	a	a	n	a
excitation (nm)	413/442	413/442	413	407
υ_{34}	183	193		
υ_{53}	200	204	197	
	218	218	217	
υ(Fe−His)	228	231		231
υ_9	255	262	270	
	283	283		
υ_{51}		310	308	
	318	317		
	328	327		
υ_8	348	347	347	347
		366		
$\delta(C_\beta C_c C_d)_{6,7}$	371	373		
$\delta(C_\beta C_c C_d)_{6,7}$	393	392	386	
$\delta(C_\beta C_a S)$	407	403	400	
$\delta(C_\beta C_a S)$	421	420	412	

[a] RR data from Hobbs et al. (1990).

located four residues after the His ligand (Figure 8) (Moore et al., 1985). Considering the differences in length of the side chain as well as in the spatial distribution and pK_a values of the nitrogen atom(s) of the Lys and Arg side chains (Richardson & Richarson, 1989), this latter suggestion appears less probable than the former to account for the quite constant frequency of the υ(Fe−His) mode of cyt *c*′(II) (Table 3).

The X-ray crystal structure of *R. molischianum* and *C. vinosum* cyt *c*′(III) indicate that minor changes are necessary to produce ionic interaction between the proximal His and the side chain of the conserved Lys residue in position X (Figure 6D). In the crystal, Lys 122 (in *C. vinosum*) or 118 (in *R. molischianum*) forms a salt bridge with an acidic residue located four residues before (Glu 126 and 122, respectively) (Ren et al., 1993). This electrostatic interaction places the Lys ϵ-nitrogen atom in front of and above the imidazole ring of His (Finzel et al., 1985; Ren et al., 1993). Taking into account the above-mentioned possibilities of protein reorganization in the proximal site of cyt *c*′, an electrostatic interaction between the axial His and the Lys residue in position X could be stabilized in solution. The decreased polarity between the protein surface and the heme pocket could also participate in the stabilization of the His−Lys ionic interaction. Finally, one may point out that a conformational movement of the conserved Lys residue between the protein surface and the proximal His would provide an effective mechanism to control the heme reactivity in relation to intermolecular interactions.

In conclusion, RR spectroscopy demonstrates that the proximal His of type a cyt *c*′(II) in aqueous solution is electronegative. The available data on the sequences and three-dimensional structures of cyt *c*′ suggest that the His ligand can electrostatically interact with a conserved basic protein residue. This interaction might be direct or through a water molecule.

Variability of the Peripheral Heme−Protein Interactions in cyt c′(II)

We have observed several spectral changes in the high- and low-frequency regions of RR spectra of cyt *c*′(II), i.e. the υ_{21} and υ_{37} modes and several low-frequency modes (Figures 3 and 4). All these alterations have been previously attributed to a difference in the heme−protein interactions. The comparison of the crystal structures of cyt *c*′(III) from *R. molischianum* and *C. vinosum* supports this conclusion. In particular, they show that residue 16, respectively a Met and a Tyr residue, influences the conformation of one of the propionate groups of heme (Ren et al., 1993). Moreover, Tyr 16 in *C. vinosum* cyt *c*′ is placed nearly parallel to the heme macrocycle and could exert a hindering effect on some out-of-plane porphyrin modes. Similar structures are expected to occur in *C. vinosum* and *R. sphaeroides* cyt *c*′ since an aromatic residue is conserved in the polypeptide sequence of *R. sphaeroides* cyt *c*′ (Phe 14) (Ambler et al., 1981).

Coordination and Spin States of Type I Ferricytochromes c′

The RR spectra of neutral cyt *c*′(III) from *R. palustris*, *R. rubrum*, and *C. vinosum* showed a single band at ca. 1501 and 1637 cm^{-1} for the υ_3 and υ_{10} modes, respectively (Strekas & Spiro, 1974; Kitagawa et al., 1977; Hobbs et al., 1990). Using Soret excitations, the υ_3 and υ_{10} regions of the RR spectra of type I cyt *c*′(III) from *R. molischianum* clearly exhibit split bands at 1494 and 1501 cm^{-1} and 1627 and 1635 cm^{-1}, respectively (Figure 1, Table 1). The RR spectra of type I cyt *c*′(III) from *R. sphaeroides* differ and show a major contribution for the 1502 and 1635 cm^{-1} bands (Figure 2). This difference in the relative contribution of the HS signal cannot be related to different pK_a values of the type I → type II transition of the two cytochromes (Moore et al., 1982; Moore & Pettigrew, 1990; Meyer & Cusanovich, 1985; La Mar et al., 1990). One may add that the spectrum of *C. vinosum* cyt *c*′ closely resembles that of *R. sphaeroides*. Indeed, major bands were reported at 1502 and 1637 cm^{-1}, but they exhibited asymmetric shapes toward their low-frequency sides, where shoulders at ca. 1493 and 1629 cm^{-1} are also distinguishable [see Figure 1 in Hobbs et al. (1990)]. This observation suggests that cyt *c*′ from *C. vinosum* adopts a spin equilibrium close to that detected in the present study for *R. sphaeroides* cyt *c*′(III). Therefore, the use of the 413.1 and/or the 406.7 nm excitation(s) allows the detection of an equilibrium between two forms of type I cyt *c*′(III) in the RR spectra of *R. molischianum*, *R. sphaeroides*, and *C. vinosum*. At 20 °C, this equilibrium is clearly species-dependent.

Taking into account previous RR data on various complexes of ferriheme *c*, the 1494 (υ_3) and 1627 (υ_{10}) cm^{-1} components are easily assignable to a 5cHS complex (Othman et al., 1994). On the other hand, the 1500−1502 and 1635−1637 cm^{-1} frequencies are intermediate between the latter frequencies and the 1504 and 1640 cm^{-1} frequencies of 6cLS ferriheme *c* complexes (Othman, 1994; Othman et al., 1994). They could be assigned to either a 5cIS, a perturbed 5cHS, or a 6cIS compound (Strekas & Spiro, 1974; Teraoka & Kitagawa, 1980; Smulevich et al., 1994a). Considering that (i) the crystal structures of *R. molischianum*, *R. rubrum*, and *C. vinosum* cyt *c*′ correspond all to a 5c form and (ii) the type I → type II conversion does not disrupt the secondary structure of the proteins in solution (Imai et al., 1969a,b), the most likely coordination number is therefore 5 for the two components of type I cyt *c*′(III). The remaining problem is to attribute the spin state of the heme compound associated with the 1500−1502 and 1635−1637 cm^{-1} bands.

Previous studies showed that several high-frequency modes are sensitive to the spin state of the heme iron (Spiro, 1983; Kitagawa, 1988). However, RR spectroscopy, in its physical principle, is not adapted to determine directly the magnetic properties of the heme metal. Changes in spin state of the iron atom influence its bonding properties with its five or six ligands so that some reorganization in the macrocycle structure takes place (Scheidt & Gouterman, 1983). The high-frequency RR bands correspond to stretching modes of C−C and C−N porphyrin bonds. Therefore, their sensitivities to the spin state of the heme iron are indirect, although effective. For a given iron(III)−phorphyrin system, there are separated regions for the RR frequencies of the 5cHS, 5cLS, and 5cIS complexes (Spiro & Burke, 1976; Teraoka & Kitagawa, 1980). In hemoproteins, the additive protein−heme interactions can nevertheless induce some heme deformations which could provoke the broadening and, possibly, the overlapping of these frequency domains.

The perchlorate complex of ferric octaethylporphyrin is the most current example of a 5c compound stabilizing an IS state (Dolphin et al., 1977). Its RR spectrum exhibits ν_3 and ν_{10} at 1513 and 1645 cm^{-1}, respectively (Teraoka & Kitagawa, 1980). This model is however far from the biological systems by several aspects, i.e. the porphyrin type, the axial ligation, as well as the solvent conditions. All these parameters are indeed more or less able to influence the ν_3 and ν_{10} frequencies. However, ferric horseradish peroxidase stabilizes a 5cIS heme at low temperatures and possesses a histidine ligand in fifth-axial coordination (Maltempo et al., 1979). Its RR spectrum shows a ν_{10} mode at 1640 cm^{-1} (Evangelista-Kirkup et al., 1985). Since heme *c* easily takes a saddle-shaped conformation (Takano & Dikerson, 1981; Finzel et al., 1985) and considering that ν_{10} is sensitive to this out-of-plane heme distortion by shifting its frequency by about −5 cm^{-1} (Alden et al., 1989; Shelnutt et al., 1991; Othman et al., 1994), a ν_{10} frequency at 1635−1637 cm^{-1} is totally plausible for a 5cIS state of ferriheme *c*.

Finally, there is some consensus to consider that type I of *C. vinosum* cyt *c′*(III) undergoes a $S = {}^5/_2 \leftrightarrow S = {}^3/_2$ spin equilibrium (Maltempo & Moss, 1976; La Mar et al., 1990). The corresponding RR spectra specifically show major bands at 1502 and 1637 cm^{-1} (Hobbs et al., 1990). All these observations and comparisons allow us to conclude that the 1500−1502 and 1635−1637 cm^{-1} bands correspond to a 5cIS heme.

Spin Equilibrium in Type I Ferricytochromes c′

The HS ↔ IS equilibrium of cyt *c′*(III) is physiologically relevant since it has been detected *in vivo* in *Rhodobacter capsulatus* cells (Monkara et al., 1992). From our preceding discussion, it appears that RR spectroscopy can characterize the 5cHS ↔ 5cIS equilibrium of type I cyt *c′* at neutral pH and 20 °C. For *R. sphaeroides* and *C. vinosum* cyt *c′*(III), this equilibrium is displaced toward the 5cIS form while the two spin states are more equally represented for *R. molischianum* cyt *c′*(III) (Hobbs et al., 1990; Figures 1 and 2). According to Weber's model (1982), these differences in the population of 5cHS and 5cIS species suggest that a flexible protein residue could interact with the proximal His. Returning to the models presented in Figure 6 and assuming that the crystallized structure represents the 5cIS form (Weber, 1982; Finzel et al., 1985), the swinging of a basic residue may be at the origin of the 5cHS ↔ 5cIS equilibrium. The 5cHS state of type I cyt *c′*(III) would be stabilized by a His−Lys or His−H_2O−Lys electrostatic interaction and an imidazole rotation (Figure 6C,D). One may note further that the residue in the Y position is Ala, Ser, and Ser in the protein sequence of *R. molischianum*, *C. vinosum*, and *R. sphaeroides*, respectively (Ambler et al., 1981) (Figure 8). The smaller steric hindrance of the Ala side chain relative to that of the Ser residue could participate in a lowering of the energetic barrier between the 5cHS and 5cIS species.

Influences of Experimental Parameters on the Observation of a Spin Equilibrium for Type I Ferricytochrome c′

As far as the available crystal structures of cyt *c′*(III) are concerned, it is not sure that they correspond to type I. The crystals of *R. molischianum* cyt *c′* were obtained from solutions of undefined pH, and those of *R. rubrum* and *C. vinosum* were prepared from neutral solutions but containing 25−30% polyethylene glycol (Weber et al., 1981; Finzel et al., 1985; Yasui et al., 1984; Ren et al., 1993). In the latter case, Imai et al. (1969a,b) demonstrated that an increase in solvent hydrophobicity, by cosolvent addition, can destabilize type I cyt *c′*(III).

Moreover, one may provide an explanation for the apparent conflicting reports on the cyt *c′* structure obtained with different spectroscopic techniques. Two points have to be considered: the physical basis of the technique used and its experimental constraints. The plausible model proposed in Figure 6D rests on two types of electrostatic interaction modulated by a change in conformation of a basic side chain. Similar relaxation processes in protein are on a time scale ranging from pico- to nanoseconds (Moore & Pettigrew, 1990). Considering the characteristic time of the Raman scattering effect (ca. 10^{-13} s) (Stockburger et al., 1986), RR spectroscopy is perfectly able to detect the two spin states, corresponding to two different histidine interactions, as two independent entities. NMR and Mössbauer spectroscopies are expected to be not so adequate to observe such a rapid effect (Moss et al., 1968; Emptage et al., 1981; La Mar et al., 1990).

On the other hand, one can remark that methods that use concentrated solutions of protein (NMR, and susceptibility measurements) largely favor the observation of a 5cHS structure for type I cyt *c′*(III) (La Mar et al., 1990; Bertini et al., 1990; Banci et al., 1992). On the contrary, methods that investigate more dilute cyt *c′* solutions (absorption, CD, RR, and EPR) provide evidence for a 5cHS ↔ 5cIS equilibrium (Imai et al., 1969a,b; Maltempo, 1974; this work). The location of the heme binding site in the terminal segment of helix D can explain how the spectroscopic properties of cyt *c′* are sensitive to changes in solvent conditions (Imai et al., 1969a,b). This sensitivity could be extended to unspecific protein−protein interactions generated by concentrated samples. These interactions could displace the HS ↔ IS equilibrium toward the HS state in forcing the Lys side chain to remain inside the heme pocket.

Conclusion

At physiological pH, *R. molischianum* and *R. sphaeroides* cyt *c′*(III) (type I) adopt significantly different mixtures of 5cHS and 5cIS species. In the reduced state (type a), these

cytochromes *c′* show RR spectral features associated with a different environment of heme. The assignment of the (Fe−His) mode at 228−231 cm^{-1} demonstrates that the proximal histidylimidazole ring has electronegative character, most likely originating from an electrostatic interaction with a basic residue in its vicinity. A similar proximal His−Lys or His−H_2O−Lys interaction is proposed to play a crucial role in the modulation of the magnetic properties of cyt *c′*(III).

ACKNOWLEDGMENT

The authors acknowledge Dr. L. Gemeroth from M. Planck Institute (Frankfurt) for his generous gift of the *R. molischianum* strain.

REFERENCES

Alden, R. G., Crawford, B. A., Doolen, R., Ondrias, M. R., & Shelnutt, J. A. (1989) *J. Am. Chem. Soc. 111*, 2070−2072.
Ambler, R. P., Bartsch, R. G., Daniel, M., Kamen, M. D., McLellan, L., Meyer, T. E., & Van Beeumen, J. (1981) *Proc. Natl. Acad. Sci. U.S.A. 11*, 6854−6857.
Argade, P., Sassaroli, M., Rousseau, D. L., Inubushi, T., Ikeda-Saito, M., & Lapidot, A. (1984) *J. Am. Chem. Soc. 106*, 6593−6596.
Banci, L., Bertini, I., Turano, P., & Vicens Oliver, M. (1992) *Eur. J. Biochem. 204*, 107−112.
Bangcharoenpaurpong, O., Schomacker, K. T., & Champion, P. M. (1984) *J. Am. Chem. Soc. 106*, 5688−5698.
Barakat, R., & Strekas, T. C. (1982) *Biochim. Biophys. Acta 679*, 393−399.
Bertini, I., Briganti, F., Monnanni, R., Scozzafava, A., Carlozzi, P., & Materassi, R. (1990) *Arch. Biochem. Biophys. 282*, 84−90.
Bolognesi, M., Onesti, S., Gatti, G., Coda, A., Ascenzi, P., & Brunori, M. (1989) *J. Mol. Biol. 205*, 529−544.
Dasgupta, S., Rousseau, D. L., Anni, H., & Yonetani, T. (1989) *J. Biol. Chem. 264*, 654−662.
Desbois, A. (1994) *Biochimie 76*, 694−707.
Desbois, A., & Lutz, M. (1981) *Biochim. Biophys. Acta 671*, 168−176.
Desbois, A., & Lutz, M. (1992) *Eur. Biophys. J. 20*, 321−335.
Desbois, A., Lutz, M., & Banerjee, R. (1981) *Biochim. Biophys. Acta 671*, 177−183.
Desbois, A., Henry, Y., & Lutz, M. (1984a) *Biochim. Biophys. Acta 785*, 148−160.
Desbois, A., Mazza, G., Stetzkowski, F., & Lutz, M. (1984b) *Biochim. Biophys. Acta 785*, 161−176.
Dolphin, D. H., Sams, J. R., & Tsin, T. B. (1977) *Inorg. Chem. 16*, 711−713.
Ehrenberg, A., & Kamen, M. D. (1965) *Biochim. Biophys. Acta 102*, 333−340.
Emptage, M. H., Xavier, A. V., Wood, J. M., Alsaadi, B. M., Moore, G. R., Pitt, R. C., Williams, R. J. P., Ambler, R. P., & Bartsch, R. G. (1981) *Biochemistry 20*, 58−64.
Evangelista-Kirkup, R., Crisanti, M., Poulos, T. L., & Spiro, T. G. (1985) *FEBS Lett. 190*, 221−226.
Evans, S. V., & Brayer, G. D. (1990) *J. Mol. Biol. 213*, 885−897.
Finzel, B. C., Poulos, T. L., & Kraut, J. (1984) *J. Biol. Chem. 259*, 13027−13036.
Finzel, B. C., Weber, P. C., Hardman, K. D., & Salemme, F. R. (1985) *J. Mol. Biol. 186*, 627−643.
Gemeroth, L. (1993) Doctoral Thesis, Max Planck Institute, University of Frankfurt, Frankfurt, Germany.
Hashimoto, S., Teraoka, J., Inubushi, T., Yonetani, T., & Kitagawa, T. (1986) *J. Biol. Chem. 261*, 11110−11118.
Hoard, J. L. (1985) in *Porphyrins and Metalloporphyrins* (Smith, K. M., Ed.) pp 317−380, Elsevier, Amsterdam.
Hobbs, J. D., Larsen, R. W., Meyer, T. E., Hazzard, J. H., Cusanovich, M. A., & Ondrias, M. R. (1990) *Biochemistry 29*, 4166−4174.
Hori, H., & Kitagawa, T. (1980) *J. Am. Chem. Soc. 102*, 3608−3613.
Horio, T., & Kamen, M. D. (1961) *Biochim. Biophys. Acta 48*, 266−286.
Hu, S., Morris, I. K., Singh, J. P., Smith, K. M., & Spiro, T. G. (1993) *J. Am. Chem. Soc. 115*, 12446−12458.
Imai, Y., Imai, K., Sato, R., & Horio, T. (1969a) *J. Biochem. 65*, 225−237.
Imai, Y., Imai, K., Ikeda, K., Hamaguchi, K., & Horio, T. (1969b) *J. Biochem. 65*, 629−637.
Jameson, G. B., Molinaro, F. S., Ibers, J. A., Collman, J. P., Brauman, J. I., Rose, E., & Suslick, K. S. (1980) *J. Am. Chem. Soc. 102*, 3224−3237.
Kamen, M. D., & Horio, T. (1970) *Annu. Rev. Biochem. 39*, 673−700.
Kitagawa, T. (1988) in *Biological Applications of Raman Spectroscopy* (Spiro, T. G., Ed.) Vol. 3, pp 97−131, Wiley, New York.
Kitagawa, T., & Ozaki, Y. (1987) *Struct. Bonding (Berlin) 64*, 71−114.
Kitagawa, T., Ozaki, Y., Kyogoku, Y., & Horio, T. (1979) *Biochim. Biophys. Acta 495*, 1−11.
Korszun, Z. R., Bunker, G., Khalid, S., Scheidt, W. R., Cusanovich, M. A., & Meyer, T. E. (1989) *Biochemistry 28*, 1515−1517.
Kuila, D., Tien, M., Fee, J. A., & Ondrias, M. R. (1985) *Biochemistry 24*, 3394−3397.
Kunishima, N., Fukuyama, K., Matsubara, H., Hatanaka, H., Shibano, Y., & Amachi, T. (1994) *J. Mol. Biol. 235*, 331−344.
La Mar, G. N., Jackson, J. T., Dugad, L. B., Cusanovich, M. A., & Bartsch, R. G. (1990) *J. Biol. Chem. 265*, 16173−16180.
Maltempo, M. M. (1974) *J. Chem. Phys. 61*, 2540−2547.
Maltempo, M. M., & Moss, T. H. (1976) *Q. Rev. Biophys. 9*, 181−215.
Maltempo, M. M., Ohlsson, P.-I., Paul, K.-G., Petterson, L., & Ehrenberg, A. (1979) *Biochemistry 18*, 2935−2941.
McGourty, J. L., La Mar, G. N., Smith, K. M., Ascoli, F., Chiancone, E., Pandey, R. K., & Singh, J. P. (1989) *Eur. J. Biochem. 184*, 53−61.
Meyer, T. E., & Kamen, M. D. (1982) *Adv. Protein Chem. 35*, 105−212.
Meyer, T. E., & Cusanovich, M. A. (1985) *Biochim. Biophys. Acta 807*, 308−319.
Momenteau, M., Scheidt, W. R., Eigenbrot, C. W., & Reed, C. A. (1988) *J. Am. Chem. Soc. 110*, 1207−1215.
Monkara, F., Bingham, S. J., Kadir, F. H. A., McEwan, A. G., Thomson, A. J., Thurgood, A. G. P., & Moore, G. R. (1992) *Biochim. Biophys. Acta 1100*, 184−188.
Moore, G. R., & Pettigrew, G. W. (1990) in *Cytochromes c: Evolutionary, Structural and Physicochemical Aspects*, pp 27−253, Springer-Verlag, Berlin.
Moore, G. R., McClune, G. J., Clayden, N. J., Williams, R. J. P., Alsaadi, B. M., Ångström, J., Ambler, R. P., Van Beeumen, J., Tempst, P., Bartsch, R. G., Meyer, T. E., & Kamen, M. D. (1982) *Eur. J. Biochem. 123*, 73−80.
Moore, G. R., Williams, R. J. P., Peterson, J., Thomson, A. J., & Mathews, F. S. (1985) *Biochim. Biophys. Acta 829*, 83−96.
Morais, J., Palma, P. N., Frazao, C., Caldeira, J., LeGall, J., Moura, I., Moura, J. J. G., & Carrondo, M. A. (1995) *Biochemistry 34*, 12830−12841.
Moss, T. H., Bearden, A. J., Bartsch, R. G., & Cusanovich, M. A. (1968) *Biochemistry 7*, 1583−1590.
Mylrajan, M., Valli, K., Wariishi, H., Gold, M. H., & Loehr, T. M. (1990) *Biochemistry 29*, 9617−9623.
Nagai, K., Kitagawa, T., & Morimoto, H. (1980) *J. Mol. Biol. 136*, 271−289.
Oldfield, T. J., Smerdon, S. J., Dauter, Z., Petratos, K., Wilson, K. S., & Wilkinson, A. J. (1992) *Biochemistry 31*, 8732−8739.
Ondrias, M. R., Rousseau, D. L., Shelnutt, J. A., & Simon, S. R. (1982) *Biochemistry 21*, 3428−3437.
Othman, S. (1994) Doctoral Thesis, University of Paris XI-Orsay, Orsay, France.
Othman, S., Le Lirzin, A., & Desbois, A. (1993) *Biochemistry 32*, 9781−9791.
Othman, S., Le Lirzin, A., & Desbois, A. (1994) *Biochemistry 33*, 15437−15448.
Petersen, J. F. W., Kadziola, A., & Larsen, S. (1994) *FEBS Lett. 339*, 291−296.

Poulos, T. L., Edwards, S. L., Wariishi, H., & Gold, M. H. (1993) *J. Biol. Chem. 268*, 4429−4440.
Rawlings, J., Stephens, P. J., Nafie, L. A., & Kamen, M. D. (1977) *Biochemistry 16*, 1725−1729.
Ren, Z., Meyer, T., & McRee, D. E. (1993) *J. Mol. Biol. 234*, 433−445.
Richardson, J. S., & Richardson, D. C. (1989) in *Prediction of Protein Structure and the Principles of Protein Conformation* (Fasman, G. D., Ed.) pp 1−98, Plenum Press, New York.
Scheidt, W. R., & Gouterman, M. (1983) in *Iron Porphyrins* (Lever, A. B. P., & Gray, H. B., Eds.) part I, pp 89−139, Addison-Wesley, London.
Scheidt, W. R., Geiger, D. K., Lee, Y. J., Reed, C. A., & Lang, G. (1985) *J. Am. Chem. Soc. 107*, 5693−5699.
Scheidt, W. R., Osvath, S. R., & Lee, Y. J. (1987) *J. Am. Chem. Soc. 109*, 1958−1963.
Shelnutt, J. A., Medforth, C. J., Berber, M. D., Barkigia, K. M., & Smith, K. M. (1991) *J. Am. Chem. Soc. 113*, 4077−4087.
Smulevich, G., Mauro, J. M., Fishel, L. A., English, A. M., Kraut, J., & Spiro, T. G. (1988) *Biochemistry 27*, 5477−5485.
Smulevich, G., Paoli, M., Burke, J. F., Sanders, S. A., Thorneley, R. N. F., & Smith, A. T. (1994a) *Biochemistry 33*, 7398−7407.
Smulevich, G., Feis, A., Focardi, C., Tams, J., & Welinder, K. G. (1994b) *Biochemistry 33*, 15425−15432.
Song, S., Boffi, A., Chiancone, E., & Rousseau, D. L. (1993) *Biochemistry 32*, 6330−6336.
Spiro, T. G. (1983) in *Iron Porphyrins* (Lever, A. B. P., & Gray, H. B., Eds.) part II, pp 89−159, Addison-Wesley, London.
Spiro, T. G., & Burke, J. M. (1976) *J. Am. Chem. Soc. 98*, 5482−5489.
Spiro, T. G., & Li, X.-Y. (1988) in *Biological Applications of Raman Spectroscopy* (Spiro, T. G., Ed.) Vol. 3, pp 1−37, Wiley, New York.
Stavrov, S. S. (1993) *Biophys. J. 65*, 1942−1950.
Stein, P., Mitchell, M., & Spiro, T. G. (1980) *J. Am. Chem. Soc. 102*, 7795−7797.
Stockburger, M., Alshuth, T., Oesterhelt, D., & Gärtner, W. (1986) in *Spectroscopy of Biological Systems* (Clark, R. J. H., & Hester, R. E., Eds.) pp 483−535, Wiley & Sons, Chichester.
Strekas, T. C., & Spiro, T. G. (1974) *Biochim. Biophys. Acta 351*, 237−245.
Sundberg, R. J., & Martin, R. B. (1974) *Chem. Rev. 74*, 471−517.
Takano, T., & Dickerson, R. E. (1981) *J. Mol. Biol. 153*, 79−94.
Teraoka, J., & Kitagawa, T. (1980) *J. Phys. Chem. 84*, 1928−1935.
Teraoka, J., & Kitagawa, T. (1981) *J. Biol. Chem. 256*, 3969−3977.
Weber, P. C. (1982) *Biochemistry* 421, 5116−5119.
Weber, P. C., Howard, A., Xuong, N. H., & Salemme, F. R. (1981) *J. Mol. Biol. 153*, 399−424.
Yamamoto, Y., Nanai, N., Chûjô, R., & Suzuki, T. (1990) *FEBS Lett. 264*, 113−116.
Yamanaka, T. (1992) in *The Biochemistry of Bacterial Cytochromes*, pp 89−168, Japan Scientific Societies Press, Tokyo.
Yasui, M., Harada, S., Kai, Y., & Kasai, N. (1984) *J. Mol. Biol. 177*, 845−846.
Yasui, M., Harada, S., Kai, Y., Kasai, N., Kusunoki, M., & Matsuura, Y. (1992) *J. Biochem. 111*, 317−327.

BI952818G